Supporting Information

SI Materials and Methods

Mice. Animal use followed National Institutes of Health guidelines under an approved protocol. Mice were kept on a 12 h light/dark cycle under 10–50 lux of fluorescent lighting during the light cycle. Transgenic mice were generated on C57BL/6J genetic background (JAX) by inserting the *STGD3* allele of the human *ELOVL4* gene into the mouse genome, under the interphotoreceptor retinoid-binding protein (*IRBP*) promoter, as described previously (1).

Isolation and culture of primary RPE cells. Primary cultures of RPE isolated from 10- to 15-day-old WT mice were prepared as described previously (2, 3). Cells were then plated on Transwell inserts (6.5 mm) with polyester membranes (Corning, Corning, NY) for phagocytosis assays, or on glass-bottom slides (MatTek, Ashland, MA) for live-cell imaging experiments. Cells were maintained in DMEM with high glucose, 10% fetal bovine serum (FBS), 2.5 mM L-glutamine, non-essential amino acids and antibiotics (Invitrogen) for 7-10 days for phagocytosis assays, or for 3 days for live-cell imaging experiments.

Culture and transduction of ARPE19 cells. ARPE19 cells were grown at 37 ºC with 5% CO_2 in DMEM-F12 with 10% FBS, 1 mM penicillin/streptomycin (Life Technologies, Carlsbad, CA) and glutamine (Life Technologies). Cells were plated on glass coverslips, and used for phagocytosis assays when confluent. For transduction experiments, the cells were incubated with Adenovirus Type 5 (Ad5) particles containing GFP, WT Elovl4, or mutant Elovl4 (generous gift from Drs Martin-Paul Agbaga and Robert E. Anderson, Dean McGee Eye Institute) for 24 h. They were then fixed with 4% formaldehyde in 0.1 M phosphate buffer for 10 min at room temperature (RT), and immunolabeled with anti-ELOVL4 (Abcam; ab14922) and anti-HA (Abcam). The ELOVL4 antibody was raised against an N-terminal

epitope (amino acids 2-22 of human ELOVL4) and reacts with both human and mouse ELOVL4. For peptide competition, the immunizing peptide (Thermo Scientific) was preincubated with the ELOVL4 antibody for 1 h at RT before the antibody was applied to the cells.

POS phagocytosis in cell culture: Purification of POSs. Mouse POSs were isolated from dark-adapted, 3- to 4-week-old WT and TG2 mice on a C57BL/6J background, as described previously (4), with minor modifications. Briefly, POSs were isolated using a discontinuous OptiPrep 8%-10%-15% step gradient in Ringer's solution (130 mM NaCl, 3.6 mM KCl, 2.4 mM $MgCl_2$, 1.2 mM $CaCl_2$, 10 mM HEPES, adjusted to pH 7.4 with KOH, 0.02 mM EDTA). Retinas were vortexed for 4 x 10 s, followed by a 1000 rpm centrifugation for 30 s at 4°C in a Sorvall HB-4 rotor, loaded on top of the OptiPrep gradient and centrifuged for 20 min at 12,000 *g*. POSs were collected at the 10%-15% interface and diluted 3 times with Ringer's solution. POSs were counted on a hemocytometer and their concentration was adjusted to 1-5 $x10^7$ POSs/ml. For live-cell imaging, POSs were isolated from 3- to 4-week-old WT and TG2 mice on a RHO-EGFP background, following the method described above.

POS phagocytosis in cell culture: Rate of POS degradation. The ability of primary cultures of WT RPE cells to digest POSs was determined, as described previously (5, 6). Briefly, equivalent amounts of purified POSs from WT or TG2 mice were fed to RPE cells grown on Transwell inserts, and incubated for 10 min at 37 °C and 5% CO_2. Unbound POSs were then removed by extensive washing. Some cultures were fixed and processed for RHO immunofluorescence (pulse time point) while others were chased for 2 h, and then processed for immunofluorescence. The number of bound and ingested POSs were identified and distinguished from each other as described previously (6), and determined by counting immunofluorescent bodies ≥ 1 μm in diameter. Briefly, cells were washed 3 times in

PBS and blocked in blocking buffer (PBS containing 1% goat serum) and labeled with RHO rabbit polyclonal antibody (pAb01) (7, 8), followed by an Alexa 568-nm conjugated goat anti-rabbit antibody (Molecular Probes, USA) for 1 h. Cells were then washed 3 times in PBS and permeabilized with 50% ethanol for 5 min at RT. After permeabilization, cells were incubated for 1 h with a combination of pAb01 and a mouse monoclonal antibody against the C-terminal portion of RHO (1D4 antibody, Millipore, USA), followed by a 30 min incubation with anti-rabbit IgG Alexa 488-nm and anti-mouse IgG Alexa-647 conjugated secondary antibodies (Life Technologies, USA). The Transwell filters were excised and mounted with FLUORO-GEL with DAPI or Tris buffer (Electron Microscopy Sciences, USA).

Immunofluorescence of cultured RPE cells. WT RPE cells were incubated with either WT or TG2 POSs for 20 min, washed extensively to remove unbound POSs, chased for 1 h, and then fixed with 4% formaldehyde in 0.1 M phosphate buffer for 10 min at RT before being processed for immunofluorescence. After fixation, cells were blocked in 5% normal goat serum (NGS), 1% bovine serum albumin (BSA) in PBS with 0.25% Triton X-100 for 1 h at RT. Cells were then incubated for 1 h at RT with primary antibodies against RHO (monoclonal 4D2, Millipore, Temecula, CA) and RAB7A (Cell Signaling Technology) or ELOVL4 (Abcam ab14922). Finally, cells were incubated with Alexa Fluor-conjugated secondary antibodies for 1 h at RT, washed, and mounted with DAPI. Quantitative co-localization of POS-opsin and RAB7A immunolabelings was evaluated using FluoView FV1000 software (Olympus). For motor protein association, WT RPE cells were used in a phagocytosis assay, as described above, fixed with ice-cold methanol for 10 min at -20 °C, and processed for immunofluorescence using primary antibodies against RHO (pAb01) and DIC (Millipore, Temecula, CA), followed by incubation with the appropriate Alexa Fluor-conjugated secondary antibodies for 1 h at RT. RHO-DIC association was quantified by

measuring co-localization of the immunofluorescent signals as well as clustering of DIC around RHO-positive phagosomes.

Live-cell imaging of cultured RPE cells. POSs from RHO-EGFP mice that were crossed with the TG2 line were purified, and fed to cultures of WT primary mouse RPE cells for 20 min. Following this pulse, phagosomes were imaged using an UltraVIEW Spinning Disk Confocal Microscope system with a Zeiss Axiovert photomicroscope including an environment chamber. A 63x oil objective with a Numerical Aperture of 1.46 was used, and movies were taken using a Hamamatsu 5.0.2 camera. Movies were acquired with the Volocity software and processed using the Volocity and Imaris software. RPE cells grown on glass-bottom dishes were imaged at 37 °C. Movies were taken after feeding cells with POSs for 20 min and washing away unbound POSs. 90-second movies at 2.9 frames per second from 12 – 15 fields of view per condition were recorded. The experiment was repeated 3 times.

Immunofluorescence of retinal tissue. For the quantification of phagosomes in vivo, WT and TG2 mice were kept under the same light cycle. They were euthanized 0.5 h and 3 h (± 15 min) after light onset and eyes were fixed in 4% formaldehyde in 0.1 M phosphate buffer. Eyecups were incubated in sucrose (15, 20 and 30% each for 1 h at least), embedded in OCT and frozen at -80 °C until use. 10-μm cryosections were cut along the entire dorso-ventral axis, and immunolabeled with RHO pAb01. RHO-positive particles ≥ 1 μm in diameter within the RPE were counted in dorsal and ventral areas of 3 non-consecutive sections of at least 3 mice from each genotype.

For immunolocalization of ELOVL4, and the assessment of oxidative stress adducts and microglial markers, in retinal sections, eyecups were processed as above. Then, 12-μm sections were cut, and quenched for 15 min in 50 mM ammonium chloride. Sections were

blocked in 5 % NGS or normal donkey serum (NDS), 1% BSA in PBS with 0.25% Triton X-100 for 1 h at RT. They were incubated with primary antibodies against RHO (mAb4D2 or pAb01), ELOVL4 (Abcam ab14922 (N-terminal), or a rabbit pAb (C-terminal) that was kindly provided by Dr Martin-Paul Agbaga (9)), 4-hydroxynonenal (4-HNE) (Alpha diagnostic International, San Antonio, TX), oxidized phosphtidylcholine (oxPC) (Sigma-Aldrich, St. Louis, MO), or F4/80 (AbD Serotec, Raleigh, NC) at 4 °C overnight in blocking buffer, and finally with corresponding secondary antibodies conjugated to Alexa Fluor fluorophores for 1 h at RT. Sections were imaged on an FV1000 confocal microscope. Quantitative analysis was performed on images taken under identical settings, and 16-bit single optical slices were analyzed on ImageJ. Negative controls, in which incubation with the primary antibody was omitted, were processed in parallel in each case. The labeling of retinal sections with ELOVL4 antibodies was repeated a minimum of 4 times with sections from different WT or mutant mice.

Electroporation of human *ELOVL4* cDNA into murine retinas. A plasmid containing cDNA of WT human *ELOVL4* (with N-terminal FLAG tag) was purchased from GeneCopoeia. PCR-mediated site-directed mutagenesis was performed to create the 5-bp deletion (delAACTT at 790-794) that is found in the STGD3 allele. A 4 μg/μl DNA solution, containing either a WT or mutant plasmid, together with a Dendra2-expressing construct, was injected into the subretinal space of P2 Crl:CD1 (ICR) mice with a FemtoJet® 4i system (Eppendorf), and electroporated with an ECM 830 Square Wave electroporation system (BTX). The animals were euthanized at P14, and the eyes were processed as above. To detect FLAG-ELOVL4, 14-μm sections were immunolabeled with FLAG antibodies (Cell Signaling) and imaged on an FV1000 confocal microscope (Olympus).

Light microscopy. Eyes were removed and immersion-fixed in 2% formaldehyde, 2.5%

glutaraldehyde in 0.1 M cacodylate buffer. Eyecups were processed for embedment in an Epon-Araldite mixture as described elsewhere (10). Semi-thin sections (0.7 mm) were obtained along the entire dorso-ventral axis, passing through the optic nerve head, and stained with 1% toluidine blue in 1% Sodium borate. Nuclei from 4 properly aligned rows of photoreceptors were counted at 0.5-mm intervals along the section.

Electron microscopy. Mouse eyes were enucleated 1.5 h post light onset, and fixed with 4% formaldehyde and 0.2% glutaraldehyde in 0.1 M sodium cacodylate buffer at 4 °C. Eyecups were prepared as mentioned above. Samples were washed in 0.1 M sodium cacodylate buffer, gradually dehydrated with increasing levels of ethanol solutions (30-90%), and infiltrated with, and embedded in LR-white resin. Ultrathin sections (70 nm) were collected on formvar-coated nickel mesh grids, and treated with 0.1% glycine, blocked in 2% BSA, and incubated with RHO mAb4D2 in 0.1 M phosphate buffer over night at 4 ^{o}C. Grids were then washed in 0.1 M phosphate buffer, and incubated with a 12-nm gold secondary antibody (Jackson Immuno Research Labs, West Grove, PA). Contrast stain with 5% uranyl acetate in ethanol was performed for 5 min. Samples were imaged with a JEM 1200-EX (JEOL) at 80 kV at magnifications of 10,000-30,000x. Immunolabeled phagosomes were counted and assigned to one of three locations in the RPE: microvilli, apical, or basal region.

Statistical analyses. Statistical analysis was performed on GraphPad Prism 5 (La Jolla, CA). Two-tailed Student *t*-tests were used to test the probability of no significant difference between mutant and control samples. To test for three or more groups, we performed one-way ANOVA followed by Tukey's *post-hoc* test. A chi-square test was used to analyze the colocalization of RHO and RAB7A.

1. Karan G*, et al.* (2005) Lipofuscin accumulation, abnormal electrophysiology, and photoreceptor degeneration in mutant ELOVL4 transgenic mice: a model for macular degeneration. *Proc Natl Acad Sci U S A* 102(11):4164-4169.
2. Gibbs D & Williams DS (2003) Isolation and culture of primary mouse retinal pigmented epithlelial cells. *Adv. Exp. Med. Biol.* 533:347-352.
3. Gibbs D, Kitamoto J, & Williams DS (2003) Abnormal phagocytosis by retinal pigmented epithelium that lacks myosin VIIa, the Usher syndrome 1B protein. *Proc Natl Acad Sci U S A* 100(11):6481-6486.
4. Jiang M*, et al.* (2015) Microtubule motors transport phagosomes in the RPE, and lack of KLC1 leads to AMD-like pathogenesis. *J Cell Biol* 210(4):595-611.
5. Diemer T, Gibbs D, & Williams DS (2008) Analysis of the Rate of Disk Membrane Digestion by Cultured RPE Cells. *Recent Advances in Retinal Degeneration*:321-326.
6. Esteve-Rudd J, Lopes VS, Jiang M, & Williams DS (2014) In vivo and in vitro monitoring of phagosome maturation in retinal pigment epithelium cells. *Adv Exp Med Biol* 801:85-90.
7. Boesze-Battaglia K, Kong F, Lamba OP, Stefano FP, & Williams DS (1997) Purification and light-dependent phosphorylation of a candidate fusion protein, the photoreceptor cell peripherin/rds. *Biochemistry* 36:6835-6846.
8. Liu X, Udovichenko IP, Brown SDM, Steel KP, & Williams DS (1999) Myosin VIIa participates in opsin transport through the photoreceptor cilium. *J. Neurosci.* 19(15):6267-6274.
9. Agbaga MP*, et al.* (2008) Role of Stargardt-3 macular dystrophy protein (ELOVL4) in the biosynthesis of very long chain fatty acids. *Proc Natl Acad Sci U S A* 105(35):12843-12848.
10. Volland S, Esteve-Rudd J, Hoo J, Yee C, & Williams DS (2015) A comparison of some organizational characteristics of the mouse central retina and the human macula. *PLoS One* 10(4):e0125631.

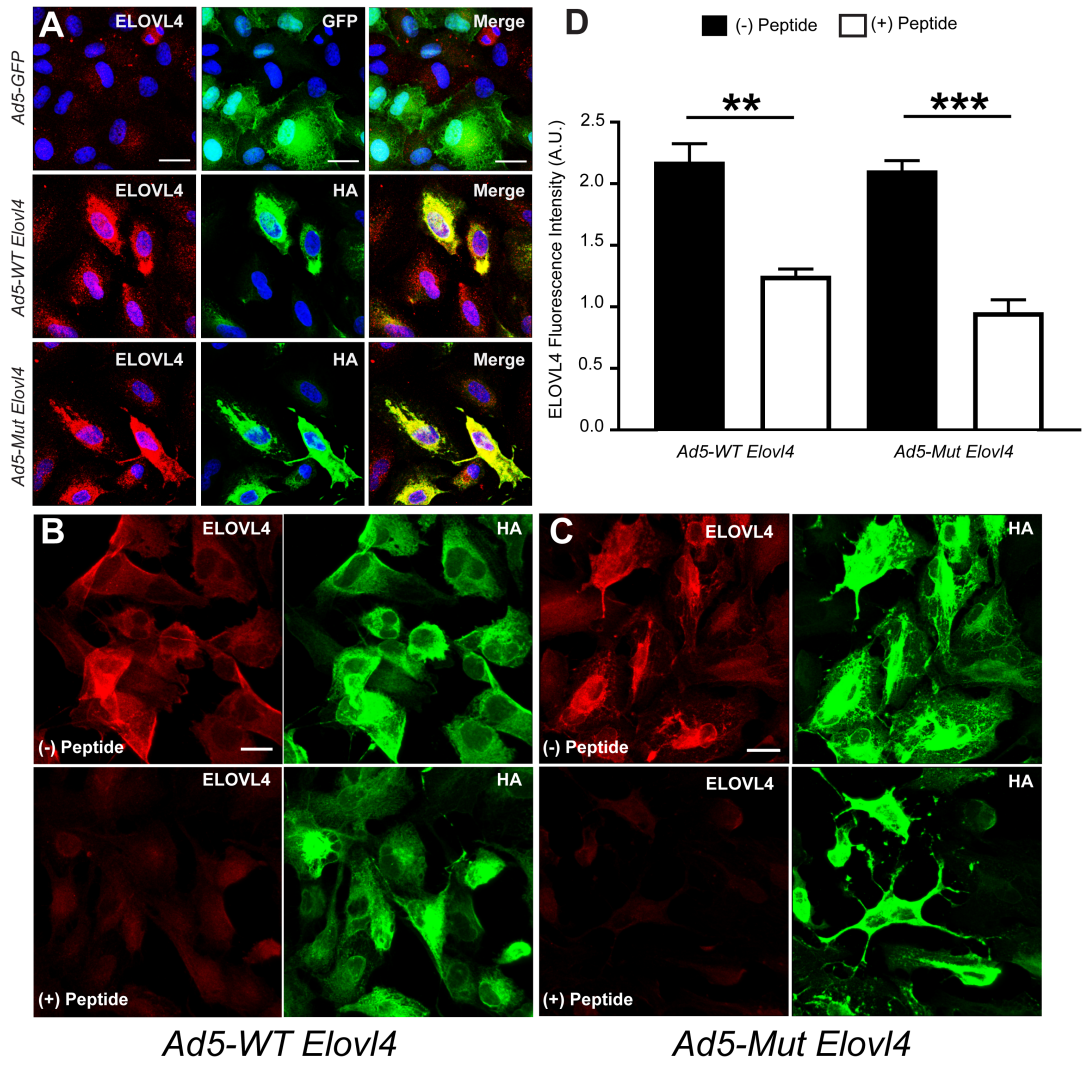

Fig. S1. Detection of WT and Mutant ELOVL4 by N-terminal ELOVL4 antibody. *(A)* ARPE-19 cells were transduced with Adenovirus Type 5 containing cDNA for GFP, HA-tagged WT or HA-tagged mutant (5-bp deletion) mouse *Elovl4*, and then labeled with the same N-terminal ELOVL4 antibody, used to immunolabel retinal sections, as in Fig. 1F. The anti-ELOVL4 shows relatively weak labeling in cells that were not transduced or transduced with GFP (top row), and very bright labeling in cells that were transduced with either HA-WT-ELOVL4 (middle row) or HA-mutant-ELOVL4 (bottom row). Moreover, immunolabeling by an HA tag antibody colocalizes with labeling by the ELOVL4 antibody. *(B, C)* To test specificity of the anti-ELOVL4, the experiment above was repeated and the immunolabeling for WT *(B)* and mutant *(C)* ELOVL4 was performed in the presence or absence of the immunizing peptide. Following 1 h preincubation with the immunizing peptide (25:1 ratio of peptide to antibody), the ELOVL4 immunolabel is significantly dimmer, even in cells that are expressing high amounts of either WT or mutant ELOVL4, as indicated by the HA immunolabel. *(D)* Quantification of mean ELOVL4 fluorescence intensity from three randomly-selected regions of ARPE19 cultures transduced with either WT or mutant ELOVL4 and immunolabeled with anti-ELOVL4 in the presence or absence of the immunizing peptide. The presence of the immunizing peptide reduces the ELOVL4 immunolabel intensity by approximately 50% in cells transduced with either WT or mutant *Elovl4*. Scale bars in (*A*-*C*) represent 20 μm. The error bars in (*D*) represent the +/- S.E.M. ** $P < 0.01$; *** $P < 0.001$.

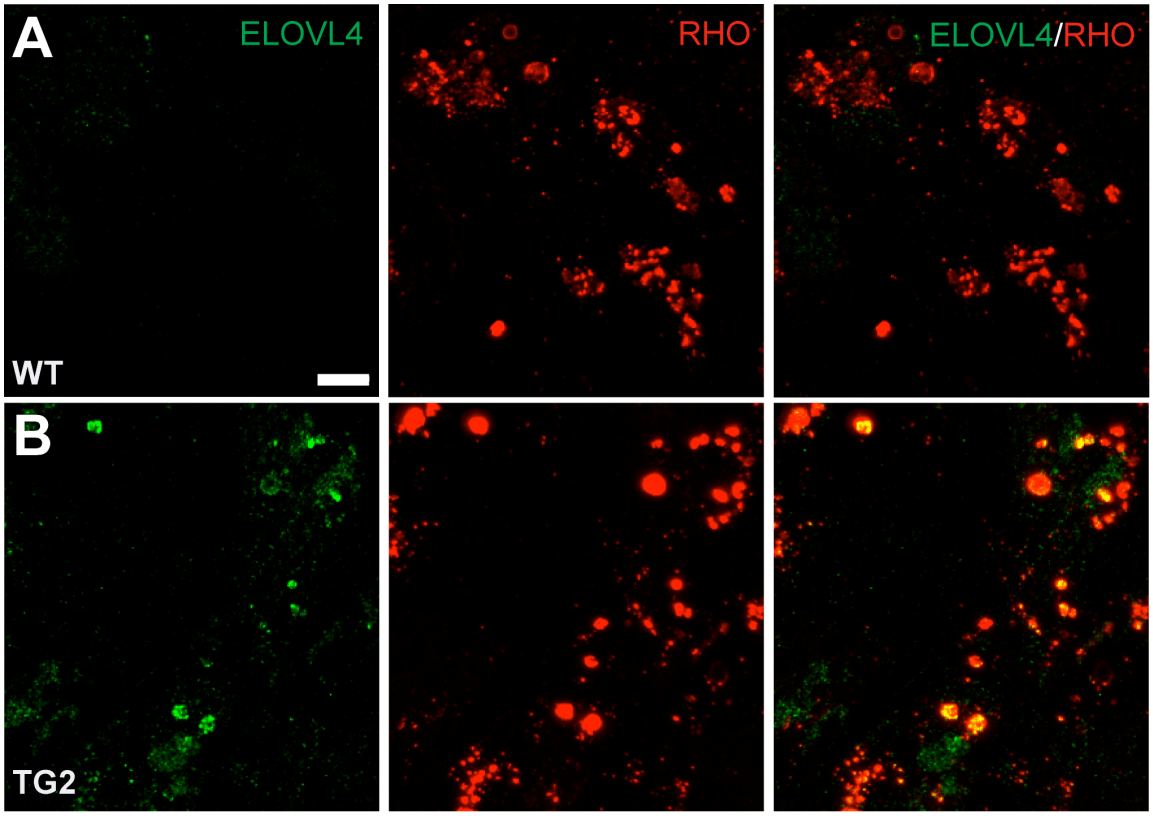

Fig. S2. Detection of ELOVL4 in TG2 phagosomes. Immunolabeling of WT primary mouse RPE cells fed WT (*A*) or TG2 (*B*) POSs, with antibodies against the N-terminal region of ELOVL4 (green) or against RHO (red). ELOVL4 is detected in RHO-positive phagosomes from TG2 POSs, but not from WT POSs. Scale bar represents 10 μm.

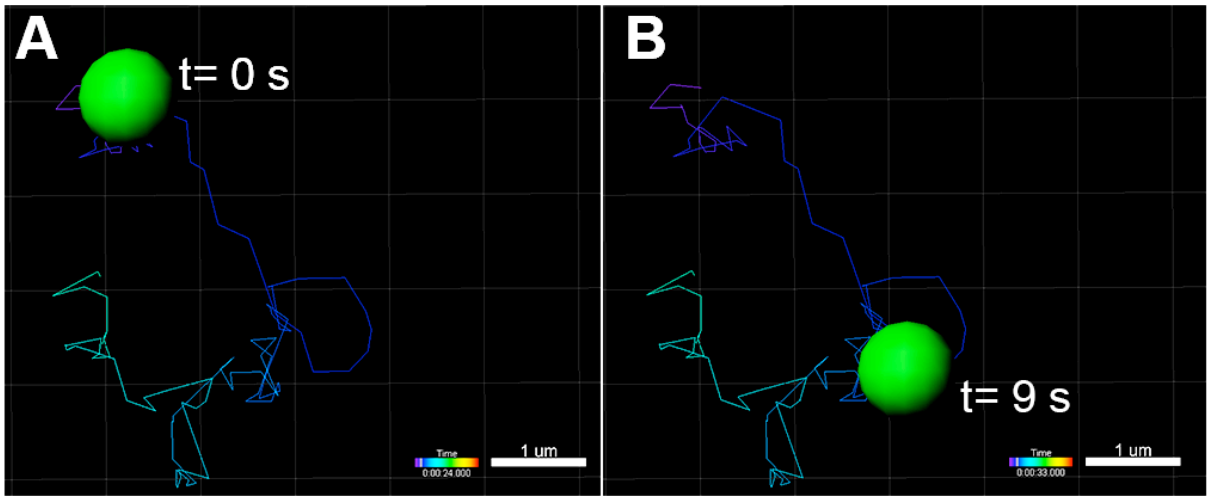

Fig. S3. Tracking and analysis of phagosome motility. (*A, B*) Snapshot images from Movie S1 at two different timepoints that are 9 seconds apart. Motility analysis revealed that the phagosome migrated a distance of approximately 3.5 μm during this 9-second interval. Scale bars in (*A*) and (*B*) represent 1 μm.

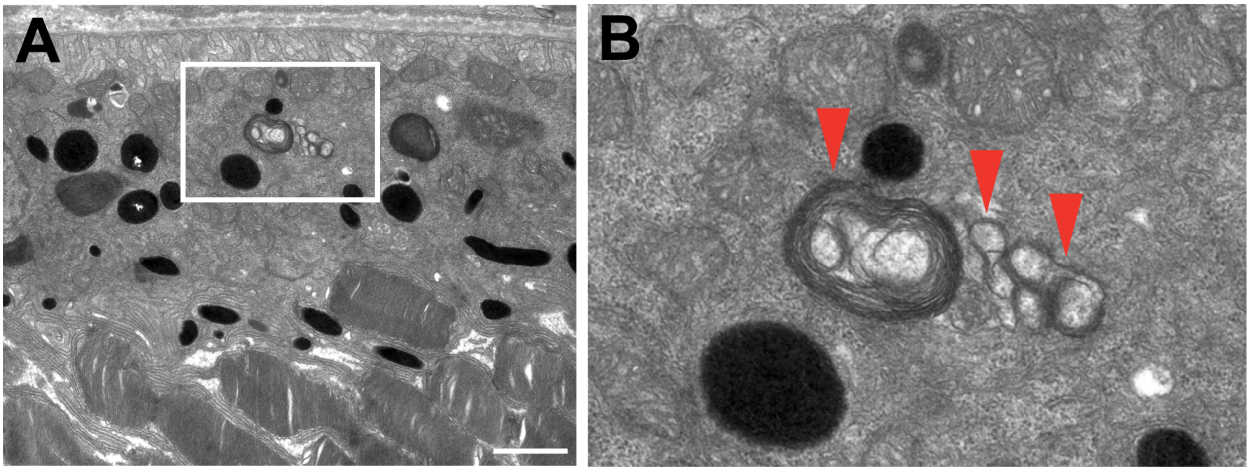

Fig. S4. Membranous debris in RPE of young TG2 mice. (*A*) Electron micrograph of retina from a TG2 animal (P21) showing membranous debris in the RPE. (*B*) An enlarged view of the region delineated by the white box in (*A*) with red arrows pointing to a cluster of these abnormal membranous structures. The scale bar in (A) represents 0.5 μm.

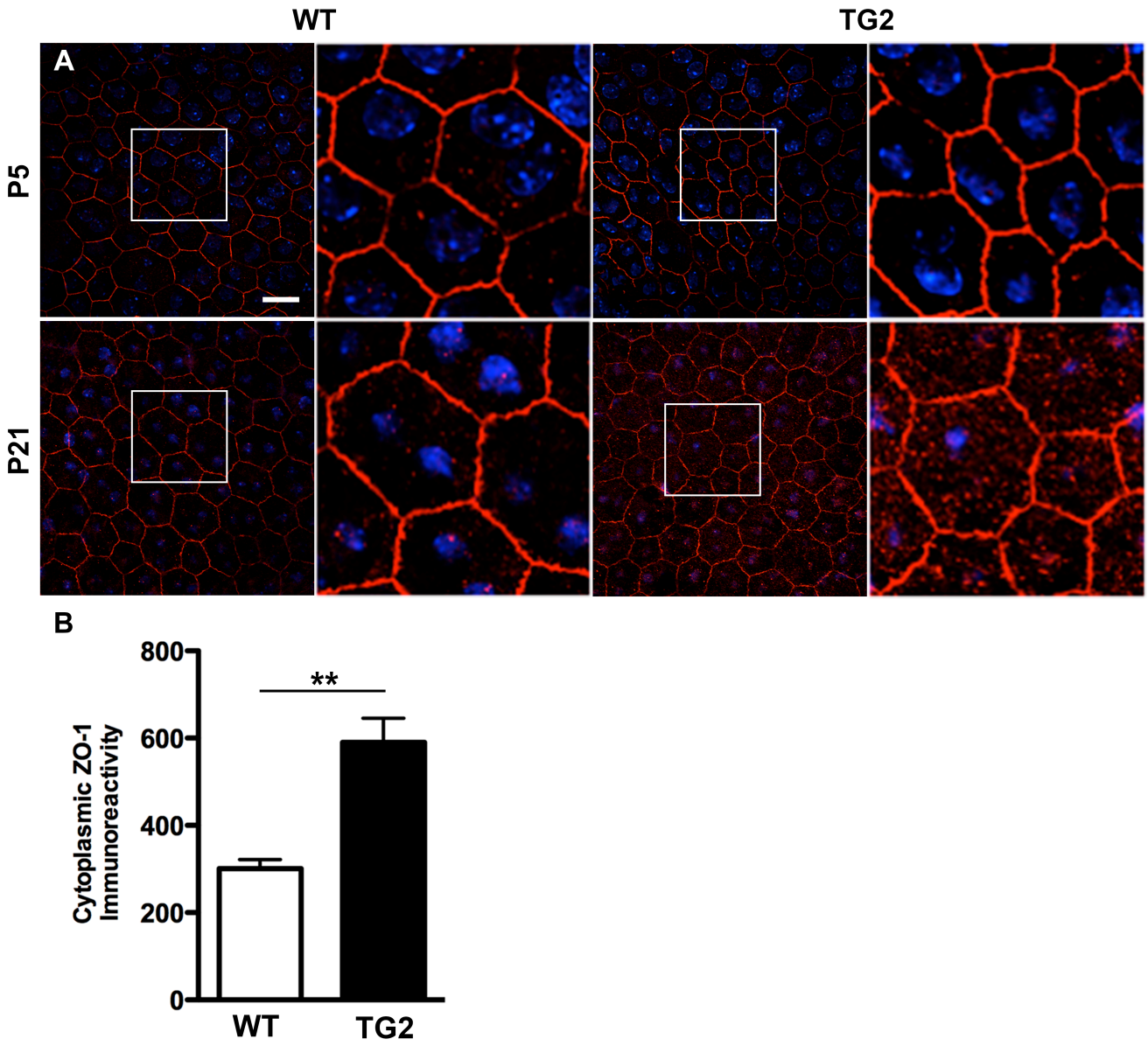

Fig. S5. Loss of ZO-1 junctional localization in TG2 RPE. (*A*) Immunolabeling of the tight junctional protein ZO-1 in RPE flatmounts from WT and TG2 animals at P5 and P21. ZO-1 labeling was similar between WT and TG2 animals at P5, whereas significantly more cytoplasmic ZO-1 was observed in TG2 RPE at P21. Enlarged views of regions delineated by white boxes in (*A*) are to the right of each corresponding panel. (*B*) Quantification of cytoplasmic ZO-1 immunoreactivity showed significantly more cytoplasmic ZO-1 in the RPE of P21 TG2 animals compared with age-matched WT littermates. The scale bar in (*A*) represents 10 μm. The error bars in (*B*) represent the +/- S.E.M. ** $P < 0.01$.

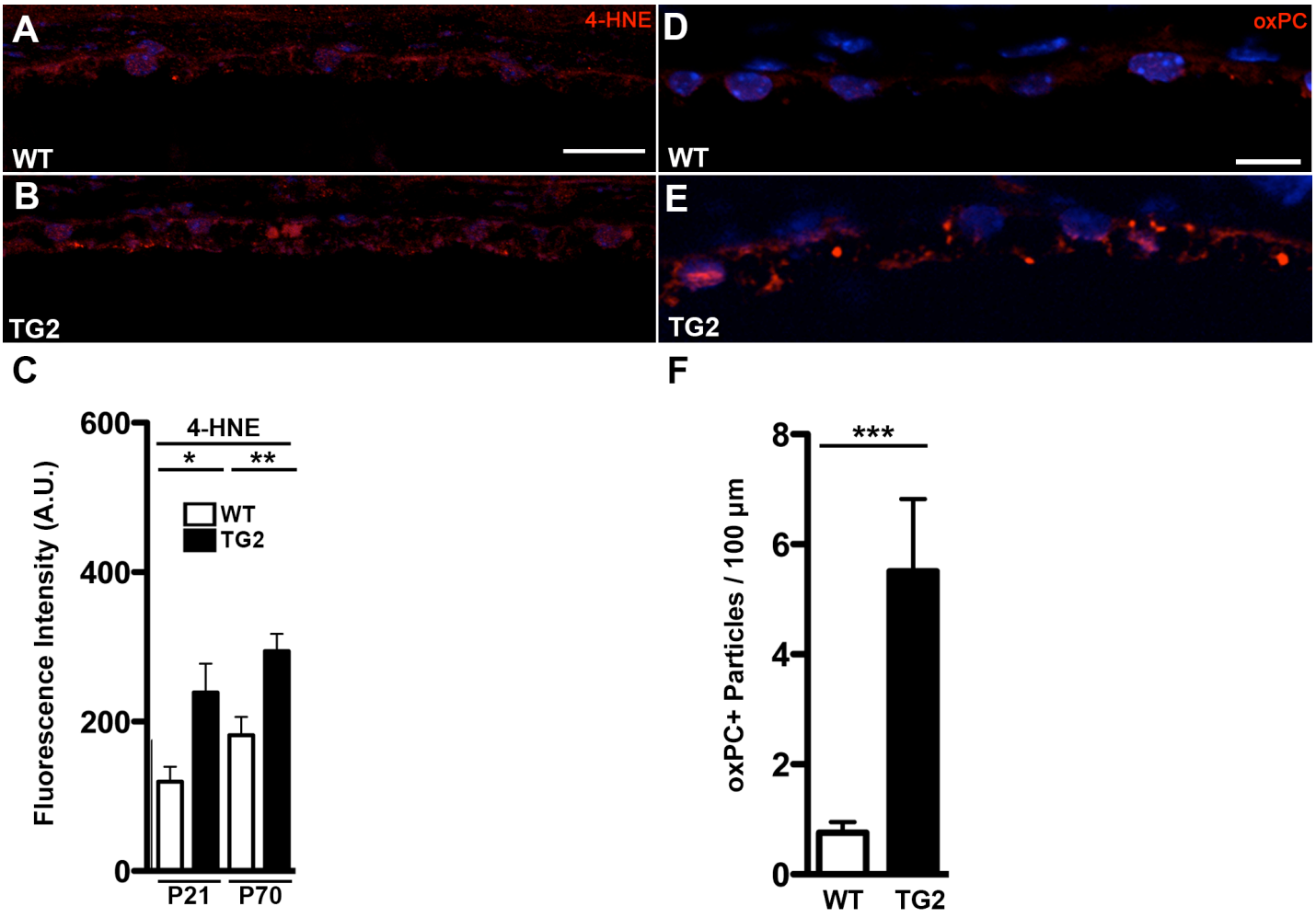

Figure S6. Increased oxidative stress in TG2 RPE. (*A-C*) Immunolabeling of retinal sections from WT (*A)* and TG2 (*B)* P70 mice for the oxidative stress marker 4-HNE (*A and B)*. (*C*) Quantification of the fluorescence intensity from the immunolabeling revealed that TG2 RPE from both P21 and P70 mice have significantly more 4-HNE relative to WT RPE of age-matched littermates. (*D, E*) Immunolabeling of retinal sections from WT (*D*) and TG2 (*E*) P70 mice for oxidized phosphotidylcholine. (*F*) Quantification of the number of oxPC-positive particles revealed more oxidized phosphotidylcholine in P70 TG2 RPE compared with WT RPE of age-matched littermates. Nuclei were counterstained with DAPI (blue). 4-HNE, 4-Hydroxynonenal; oxPC, oxidized phosphotidylcholine. The scale bars in (*A*) and (*D*) represent 10 µm. Error bars in (*C*) and (*F*) represent +/- S.E.M. * $P < .05$; ** $P < 0.01$; *** $P < 0.001$.

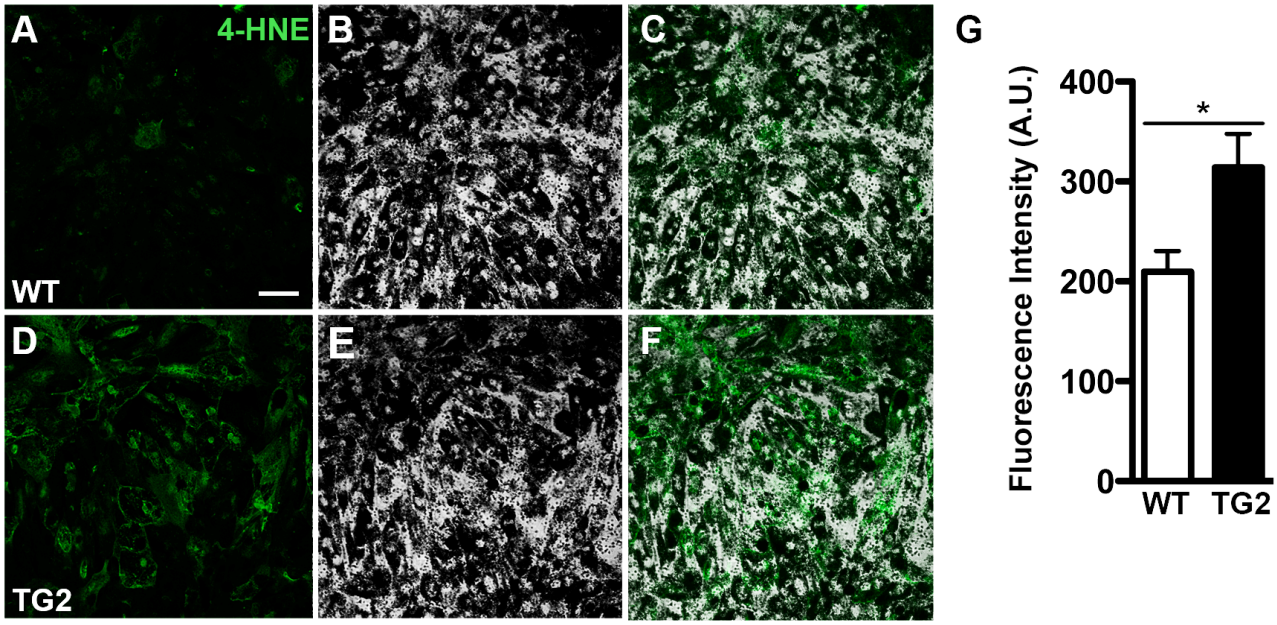

Figure S7. Increased oxidative stress in WT RPE fed TG2 POSs. (*A-F*) Primary cultures of WT RPE were incubated with WT (*A-C*) or TG2 (*D-F*) POSs for 2 h, and immunolabeled for the oxidative stress marker, 4-HNE. Phase contrast micrographs (*B, E*), merged with the immunofluorescence signal of 4-HNE (*A, D*), are shown in panels (*C*) and (*F*). (G) Quantification of the 4-HNE fluorescence signal showed that RPE cells fed TG2 POSs had significantly more 4-HNE adducts relative to those fed WT POSs. Scale bar in (*A*) represents 10 μm. Error bars in (*G*) represent +/- S.E.M. * $P < .05$.

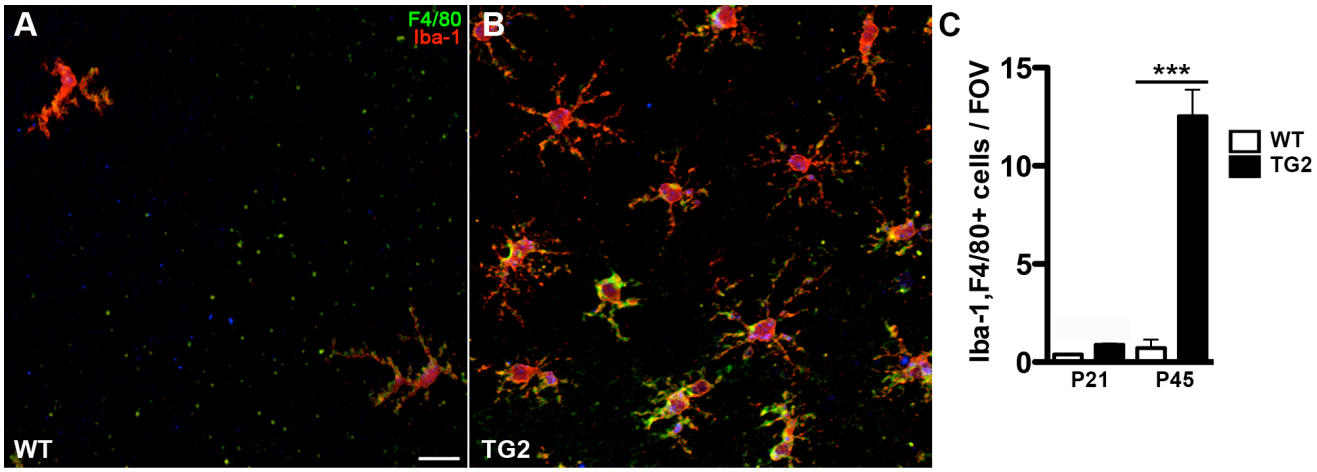

Fig. S8. Activated microglia in the retina of TG2 mice. (*A, B*) Images of retinal RPE/Choroid flatmounts, corresponding to the central region of P45 WT (*A*) and TG2 (*B*) mice, immunolabeled with antibodies against F4/80 and Iba-1, as markers for microglia. Note the significantly higher number of subretinal, activated microglial cells in the RPE/Choroid flatmounts from TG2 mice (*B*). The presence of the activated microglia in the subretinal space was observed in retinal sections. The microglia adhere to the apical surface of the RPE during the preparation of a flatmount, so that they are retained even though the neural retina has been removed. (*C*) Quantification of subretinal microglial cells positive for Iba-1 and F4/80 immunolabeling in RPE/Choroid wholemounts of P21 and P45 WT and TG2 mice (ANOVA with Tukey's post-hoc test, ***, $P < 0.0001$. n=3 animals /group at P21 and n=5 animals/group at P45). FOV, field of view. Scale bar in (*A*) represents 10 μm. Error bars in (*C*) represent +/- S.E.M. *** $P < 0.001$.

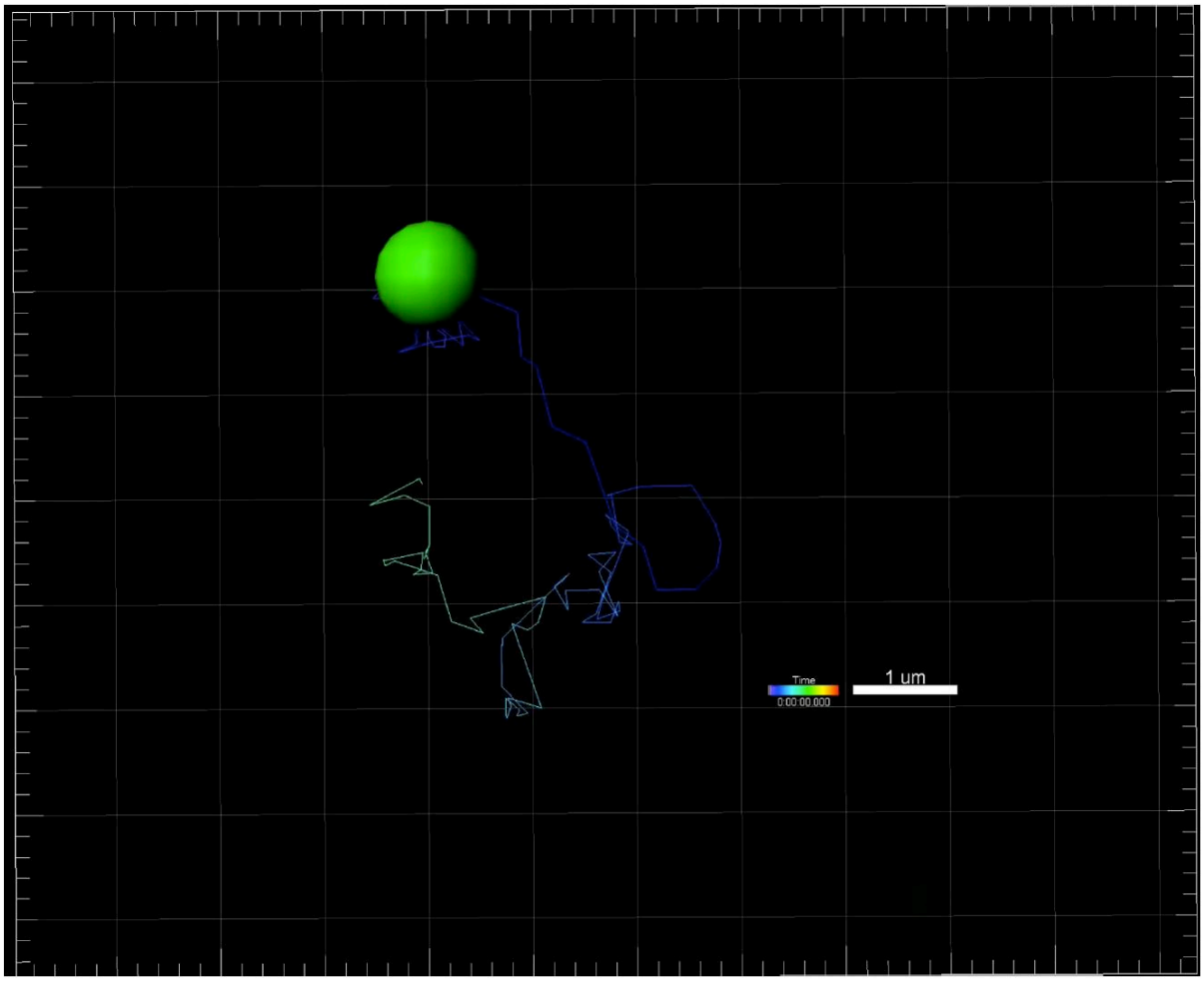

Movie S1. Phagosome motility in live RPE. A phagosome derived from RHO-EGFP POSs can been seen moving inside a cultured WT RPE cell; the phagosome is replaced with a green spot using the Imaris software for ease of visualization. Phagosome motility was tracked for 107 s. The movie was captured at 2.9 frames per second using a spinning disk confocal microscope, and plays at 5 frames per second. The color of the track indicates how far in time the phagosome is in respect to the 107-second movie. Scale bar represents 1 μm.